SCIENTIFIC REPORTS

OPEN

SUBJECT AREAS:
PATHOGENS
ENZYMES
GLYCOBIOLOGY

Received
24 June 2014

Accepted
17 September 2014

Published
24 October 2014

Correspondence and requests for materials should be addressed to N.E. (numenius@cnc.uc.pt)

* These authors contributed equally to this work.

Mycobacterium hassiacum recovers from nitrogen starvation with up-regulation of a novel glucosylglycerate hydrolase and depletion of the accumulated glucosylglycerate

Susana Alarico[1]*, Mafalda Costa[1]*, Marta S. Sousa[1], Ana Maranha[1], Eva C. Lourenço[2], Tiago Q. Faria[1], M. Rita Ventura[2] & Nuno Empadinhas[1,3]

[1]CNC – Center for Neuroscience and Cell Biology, University of Coimbra, Portugal, [2]ITQB – Instituto de Tecnologia Química e Biológica, Oeiras, Portugal, [3]III/UC – Institute for Interdisciplinary Research, University of Coimbra, Portugal.

Some microorganisms accumulate glucosylglycerate (GG) during growth under nitrogen deprivation. However, the molecular mechanisms underlying the role of GG and the regulation of its levels in the nitrogen stress response are elusive. Since GG is required for biosynthesis of mycobacterial methylglucose lipopolysaccharides (MGLP) we examined the molecular mechanisms linking replenishment of assimilable nitrogen to nitrogen-starved *M. hassiacum* with depletion of GG accumulated during nitrogen deficiency. To probe the involvement of a newly identified glycoside hydrolase in GG depletion, we produced the mycobacterial enzyme recombinantly and confirmed the specific hydrolysis of GG (GG hydrolase, GgH) *in vitro*. We have also observed a pronounced up-regulation of GgH mRNA in response to the nitrogen shock, which positively correlates with GG depletion *in vivo* and growth stimulation, implicating GgH in the recovery process. Since GgH orthologs seem to be absent from most slowly-growing mycobacteria including *M. tuberculosis*, the disclosure of the GgH function allows reconfiguration of the MGLP pathway in rapidly-growing species and accommodation of this possible regulatory step. This new link between GG metabolism, MGLP biosynthesis and recovery from nitrogen stress furthers our knowledge on the mycobacterial strategies to endure a frequent stress faced in some environments and during long-term infection.

Nitrogen is the most abundant element in the Earth's atmosphere and ranks fourth in the planet's biomass[1]. Most atmospheric nitrogen is found in the form of dinitrogen (N_2), which is inaccessible to eukaryotes and most prokaryotes. The environmental availability of assimilable (reactive) nitrogen is an essential requisite for bacterial growth and biomass generation through incorporation in DNA, RNA, proteins and cell wall components[2]. Although some bacteria evolved nitrogenases for the fixation of atmospheric nitrogen (diazotrophy) into readily assimilable ammonium, the large majority of bacteria, including members of the genus *Mycobacterium*, can only assimilate ammonium or other nitrogenous sources such as nitrate or nitrite[3]. There are anecdotal reports of nitrogen-fixing mycobacteria but typical nitrogenase genes have not been detected in the genomes available[4,5]. Most mycobacteria are saprophytes with a broad spectrum of environmental adaptation but many can also opportunistically infect humans[6,7]. The time required to form visible colonies on agar medium traditionally divides mycobacteria into slowly-growing mycobacteria (SGM) and rapidly-growing mycobacteria (RGM)[8]. Most pathogenic mycobacteria, including *M. tuberculosis* and *M. leprae* belong to the SGM group, while RGM are typically environmental species.

In order to adapt to environmental nitrogen scarcity, bacteria rely on diverse mechanisms to ensure its acquisition, assimilation while coordinating the nitrogen stress response[2,9]. In *M. smegmatis*, nitrogen stress has been shown to impact growth rate, metabolism and global gene expression programs including up-regulation of genes for energy generation and of pathways for scavenging carbon and alternative nitrogen sources[2,3]. In addition, this organism has recently been found to progressively accumulate glucosylglycerate (GG) during

adaptation to nitrogen deprivation[10]. This organic solute was also found to accumulate in a few unrelated bacteria enduring combined osmotic stress and nitrogen scarcity[11–13].

Glucosylglycerate was initially identified in the reducing end of a polysaccharide isolated from *M. phlei* and *M. tuberculosis* designated methylglucose lipopolysaccharide (MGLP) due to its high content in methylglucose and a low level of esterifications with short-chain fatty acids[14]. Free GG detected in *M. smegmatis* extracts was considered the primer for initiation of MGLP biosynthesis[15]. This amphiphilic polysaccharide has been detected in all mycobacterial strains examined thus far and proposed to modulate fatty acids synthesis *in vivo*[15–18]. A similar polymethylated polysaccharide (PMPS) of methylmannose (MMP) lacking GG and lateral acyl groups has also been identified in mycobacteria but, so far, only RGM have been shown to produce this MGLP-related macromolecule[19]. Despite the fact that GG has been identified over half-century ago, only recently have the enzymes involved in this solute's biosynthesis been identified[13]. In mycobacteria, GG is synthesized as a phosphorylated precursor by a glycosyl-3-phosphoglycerate synthase (GpgS) and dephosphorylated by a glycosyl-3-phosphoglycerate phosphatase (GpgP)[20,21]. Disruption of the *M. smegmatis gpgS* not only dramatically affected MGLP levels and the organism's ability to endure thermal stress, but also slightly affected its growth rate and ammonium uptake rate in nitrogen-limited medium, corroborating the crucial link between GG metabolism, nitrogen assimilation and *M. smegmatis* fitness[10,22]. The *M. tuberculosis gpgS* gene was proposed to be essential for growth[23].

Although important roles for GG in microbial physiology have been recognized, the metabolic pathways where it intervenes are mostly enigmatic. Recently, a glycosyl hydrolase able to hydrolyze mannosylglycerate (MG), a GG-related osmolyte common in hyperthermophilic archaea and some thermophilic bacteria, was identified in *Thermus thermophilus* and designated mannosylglycerate hydrolase (MgH)[24]. Despite the fact that this organism only accumulates MG and not GG, MgH was also shown to efficiently hydrolyze GG, as were the functional MgHs detected in *Rubrobacter radiotolerans* and in the primitive plant *Selaginella moellendorffii*[25].

Mycobacterium hassiacum was isolated from human urine and from a peritoneal dialysis peritonitis patient and is, so far, the most thermophilic member in the genus[26–28]. Herein, we identified the putative mycobacterial MgH ortholog, expressed the corresponding gene recombinantly and begun to investigate the fate of GG accumulated during growth in nitrogen-poor medium. We confirmed that the mycobacterial *mgH* homolog encodes a novel and highly specific GG hydrolase (GgH), whose orthologs are almost exclusively restricted to RGM[29]. The high levels of intracellular GG in *M. hassiacum* grown under nitrogen limitations were dramatically depleted in response to a sudden source of nitrogen, accompanied by a pronounced up-regulation of *ggH* expression. Our results associate GgH to GG hydrolysis and provide an important contribution to the understanding of the sequence of events in the global responses of mycobacteria to nitrogen stress, toward clarification of the role of GG during nitrogen starvation and recovery. Our data also raise new questions about the biosynthesis and the physiological role of MGLP in mycobacteria facing nitrogen deprivation.

Results

Growth of *M. hassiacum* in complex and nitrogen-restricted media. *Mycobacterium hassiacum* is a rapidly-growing mycobacterium (RGM) that grows between 30 and 65°C[27,29], with maximal growth rate at 50°C. The specific growth rate (μ) of *M. hassiacum* in GPHF medium at 50°C was 0.227 ± 0.021 h^{-1}, calculated up to an OD_{610nm} ~ 7.0–8.0 (corresponding to 48–50 h growth) since beyond this density cells aggregate (Fig. 1). The specific growth rate at 37°C in this medium was 0.038 ± 0.002 h^{-1}, about 6-fold lower than at 50°C (Fig. 1). Growth rate under nitrogen-deficient conditions calculated from the exponential phase alone was 0.089 ± 0.023 h^{-1} (Fig. 1). After the 72 h point the control culture continued to grow at μ = 0.007 ± 0.002 h^{-1} while supplementation with ammonium stimulated the growth rate 3-fold to μ = 0.019 ± 0.001 h^{-1}. The ammonium-supplemented culture could reach an OD_{610} of 4.03 after 6 days, while the nitrogen-exhausted culture did not grow beyond an OD_{610} of 2.76 in the same period (Fig. 1).

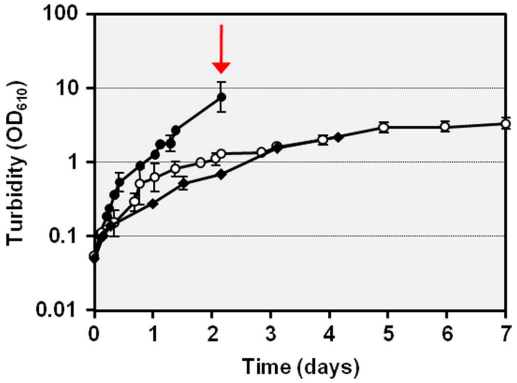

Figure 1 | Growth of *M. hassiacum* in rich GPHF medium at 50°C (●, μ = 0.227 ± 0.021 h^{-1}) and at 37°C (◆, μ = 0.038 ± 0.002 h^{-1}), and in nitrogen-restricted modified Middlebrook 7H9 medium (○, μ = 0.089 ± 0.023 h^{-1}). Growth rates reflect early exponential phases of growth. The growth rate between 2–7 days in the non-supplemented curve was 0.007 ± 0.002 h^{-1}. The arrow indicates the turbidity above which cells aggregate. The growth curves were obtained from the mean values of three independent experiments.

Quantification of intracellular GG in *M. hassiacum*. Qualitative analysis by TLC clearly demonstrated that GG gradually accumulate as the growth proceeds in nitrogen-limited conditions (Fig. S1). This culture was supplemented with 10 mM of $(NH_4)_2SO_4$ at 72 h growth, when the level of GG was close to the highest detected. Supplementation with 10 mM $(NH_4)_2SO_4$ elicited a dramatic depletion of GG levels as measured after 4, 24 and 48 h, while in the corresponding extracts from nitrogen-exhausted cultures, GG levels increased for further 4 hours and begun to gradually decrease during the time analyzed (Fig. 2 and Fig. S1). The GG : glucose (1 : 1) stoichiometry justified utilization of the MgH from *R. radiotolerans* and of the GgH characterized in this study to accurately quantify the GG accumulated at all phases of *M. hassiacum* growth (Fig. 2).

GgH sequence analysis, phylogeny and genomic environment. The genome of *M. hassiacum* DSM 44199 was recently sequenced, which allowed the identification of a protein sequence with significant amino acid identity (>30%) to mannosylglycerate hydrolases (MgHs) from two thermophilic bacteria[24,29]. The 1341 bp gene, herein designated *ggH*, encodes a 446 amino acid polypeptide with a calculated molecular mass of 50.8 kDa and a theoretical isoelectric point of 6.11. BLAST searches with the GgH sequence revealed a conserved domain of glycoside hydrolases classified within the family 63 (GH63) whose catalytic residues are unidentified (CAZY database, www.cazy.org)[30]. The closest homologs of *M. hassiacum* GgH shared different amino acid identities with those from other RGM species (except *M. tusciae* and *M. vulneris*) ranging from 81 to 89% (Table 1), followed by orthologs in the related *Nocardia* (78–79%), *Rhodococcus* (77–79%) and *Gordonia* (74–78%) (Fig. 3). GgH homologues could not be detected in most SGM with genomes available (Table 1). Distantly related homologues were detected in *T. thermophilus* (MgH, 36%), *R. radiotolerans* (MgH, 34%) and in *Rhodothermus marinus* (two

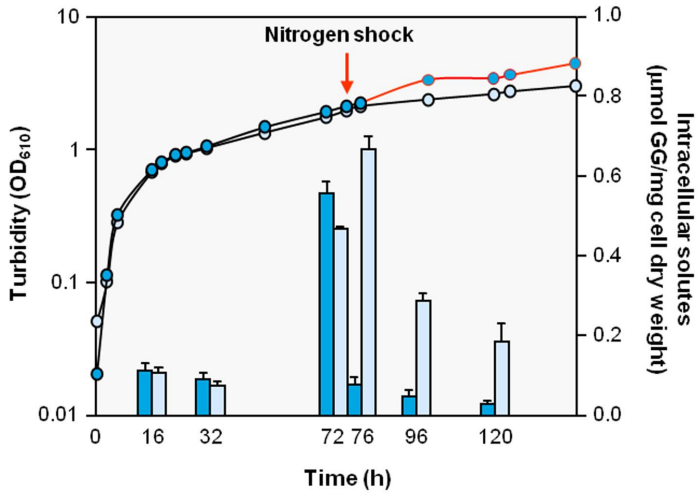

		Nitrogen shock	Nitrogen limited
Sampling	Time (h)	µmol GG/mg cell dry weight	µmol GG/mg cell dry weight
(OD_{610}=0.6)	16	0.100±0.034	0.150±0.037
(OD_{610}=1.0)	32	0.111±0.019	0.097±0.020
(OD_{610}=2.0)	72	0.582±0.005	0.579±0.004
(4h)*	76	0.098±0.035	0.782±0.016
(24h)*	96	0.061±0.002	0.398±0.011
(48h)*	120	0.039±0.007	0.146±0.008

Figure 2 | (A) Intracellular GG levels in *M. hassiacum* during growth under nitrogen-restricted medium. One culture (dark blue) was supplemented with a rich source of nitrogen (10 mM ammonium sulphate) at a specific time point (red arrow, nitrogen shock). Growth rate stimulation elicited by the nitrogen shock is indicated by the red line. (B) Sampling points and GG levels in *M. hassiacum* cells cultured under nitrogen stress and after ammonium supplementation. The inset highlights the 6-fold decrease in GG levels elicited by ammonium replenishment (red line). *, sampling time after the nitrogen shock.

orthologs with 34% and 41%). Among the organisms known to produce GG, in addition to mycobacteria and nocardia, GgH orthologs could only be detected in the bacterium *Persephonella marina* (36%) (Table 2). The genomes of the GG-producing *Streptomyces caelestis* and *Streptomyces lincolnensis* are not available but GgH orthologs are widely distributed across *Streptomyces* species[31,32] (Fig. 3). The genome of the halophilic archaeon *Methanohalophilus portucalensis* where GG has been detected, was also not available but the related species *Methanohalophilus mahii* lacks a GgH homolog[33]. GgH homologs are also absent from other GG-accumulating organisms namely the marine cyanobacteria *Synechococcus* PCC7002 and *Prochlorococcus marinus*, the halophilic bacterium *Halomonas elongata* (*Cromohalobacter salexigens*), the plant pathogen *Erwinia chrysanthemii* (*Dickeya dadantii*) and the desiccation-resistant *Geodermatophilus obscurus*[13] (Table 2).

The group including GgHs from *T. thermophilus*, *R. radiotolerans*, *P. marina* and *R. marinus* is heterogeneous and forms a distinct cluster separated from actinobacterial GgHs, which indicates a more distant phylogenetic relationship (Fig. 3). The *ggH* genomic context analyses confirmed that the regions flanking *ggH* have similar organization in *M. hassiacum* and *M. smegmatis* (Fig. 4). On the other hand, the corresponding region in *M. tuberculosis* lacks *ggH* and additional genes annotated as putative components of a transport system (Fig. 4).

Purification, oligomerization and substrate specificity of the recombinant GgH. The highly expressed and bioactive recombinant His-tagged GgH was purified to homogeneity in one step with a Ni-Sepharose column (Fig. S2) and 40% buffer B (see Methods). The recombinant GgH behaved as a dimeric protein in solution, with a molecular mass of about 108.9 ± 2.6 kDa, as determined by analytic size-exclusion chromatography (results not shown).

Among the substrates tested, and unlike the GG-hydrolyzing MgHs from *T. thermophilus* and *R. radiotolerans*, the GgH was only able to efficiently hydrolyze GG into glucose and glycerate. Trace activity was detected in assays with the related sugar mannosylglycerate (MG), but only after 1 h incubation at 42°C (not shown). The release of nitrophenol from synthetic 4-nitrophenyl-α-D-glucopyranoside and 4-nitrophenyl-β-D-glucopyranoside was not detected. The enzyme was unable to catalyze transglucosylation reactions in the presence of high concentrations of GG or of GG plus glucose, even when the mixtures were incubated for 24 h.

Properties of GgH. Biochemical and kinetic parameters of GgH were determined from the glucose released from GG hydrolysis as described in the Methods section. Under the conditions tested, GgH was optimally active at 42°C, with nearly undetectable activity below 25°C and only about 38% of maximal activity at 55°C (Fig. 5A). Half-life values for inactivation of GgH at 37, 42 and 50°C were 63.6 ± 18.0 h, 15.7 ± 1.2 h and 0.4 ± 0.2 h, respectively (Fig. 5B). At 50°C the enzyme was unstable as the residual activity decreased abruptly during the initial 2 h incubation (Fig. 5B). After this period, the activity remained constant and GgH retained about 30% maximal activity during the 24 h tested.

Table 1 | Identification of *ggH*, *gpgS* and *gpgP* orthologs in the available genomes from *Mycobacterium* species and correlation with the presence of MMP and MGLP

	Genes			PMPSs detected			
Mycobacterium spp.	*gpgS*	*gpgP*	*ggH*	MGLP	MMP	Growth	References
M. tuberculosis *	●	●	○	●	○	SGM	17
M. bovis BCG	●	●	○	●	○		56
M. leprae *	●	●	○	●	○		57
M. canettii	●	●	○	-	-		-
M. ulcerans	●	●	○	-	-		-
M. avium	●	●	○	-	-		-
M. intracellulare	●	●	○	-	-		-
M. marinum	●	●	○	-	-		-
M. xenopi *	●	●	○	●	○		58
M. vulneris	●	●	●	-	-		-
M. tusciae	●	●	●	-	-	SGM/RGM	
M. indicus pranii	●	●	○	-	-	RGM	-
M. hassiacum	●	●	●	-	-		-
M. abscessus	●	●	●	-	-		-
M. chubuense	●	●	●	-	-		-
M. gilvum	●	●	●	-	-		-
M. vanbaalenii	●	●	●	-	-		-
M. thermoresistibile	●	●	●	-	-		-
*M. phlei**	●	●	●	●	●		19,59
*M. smegmatis**	●	●	●	●	●		15,59
M. parafortuitum	-	-	-	●	●		59
*M. aurum**	-	-	-	●	●		59

(●) Highly conserved sequences (70–100% amino acid identity) or polymethylated polysaccharides (PMPSs) detected.
(○) Absence of conserved sequences or PMPSs not detected.
(-) No information available.
(*) The authors examined clinical isolates or strains that are no longer available.
SGM, slowly-growing mycobacteria; RGM, rapidly-growing mycobacteria; GpgS, glucosyl-3-phosphoglycerate synhase[20]; GpgP, glucosyl-3-phosphoglycerate phosphatase[21]; GgH, glucosylglycerate hydrolase.

The enzyme was active between pH 4.0 and 7.0 and maximally at pH 5.8 (in sodium phosphate buffer) although citrate-phosphate buffer (pH 2.6–5.0) inhibited GgH activity (Fig. 5C).

The activity was not dependent on divalent cations, but Mg^{2+} enhanced the activity with maximal stimulation achieved with 5 mM (~111%). Other divalent cations tested, namely Co^{2+}, Cu^{2+}, Fe^{2+} and Zn^{2+} ions were inhibitory whereas Mn^{2+} and Ca^{2+} did not affect GgH activity (Fig. 6). The purified GgH was only stable in the presence of high concentrations of KCl (>50 mM) in sodium phosphate buffer, and the stimulatory effect of variable KCl concentrations on the enzyme activity was shown to be maximal with 100 mM KCl (Fig. 6).

The enzyme exhibited Michaelis-Menten kinetics at 37, 42 and 50°C under optimal pH conditions. Kinetic parameters (K_M and V_{max}) for GG hydrolysis at 37°C and 42°C were comparable and slightly higher at 50°C (Table 3).

Transcriptional analysis of *ggH* expression. RNA extraction from *M. hassiacum* cells yielded samples with 280/260 ratios between 1.8 and 2 indicating good quality[34]. All RNA concentrations were normalized prior to cDNA synthesis. Primers' efficiencies were calculated and the values were 101%, which are in the expected range[34]. The *ggH* expression analyses were performed by RT-qPCR and only the samples without primer and genomic DNA contamination were used. For assessment of the relative expression of *ggH* the Livak method was used and the $2^{-\Delta\Delta Ct}$ were calculated as previously described[35]. The results obtained showed a significant increase in the expression of *ggH* four hours after the addition of 10 mM ammonium sulphate (nitrogen shock) to the growth medium (Fig. 7). This increased levels of *ggH* transcripts decreased over time since 48 h after the nitrogen shock mRNA levels were comparable to those measured at the early exponential phase of growth.

Discussion

The emergence of multidrug-resistant tuberculosis (TB) and also of atypical infections by nontuberculous mycobacteria (NTM) calls for intense research on the exceptional ecological, physiological and metabolic traits of these pathogens, many of which with a wide spectrum of environmental adaptation[6,10]. The mycobacterial lipid-rich cell envelope is critical in their adaptation to adverse conditions

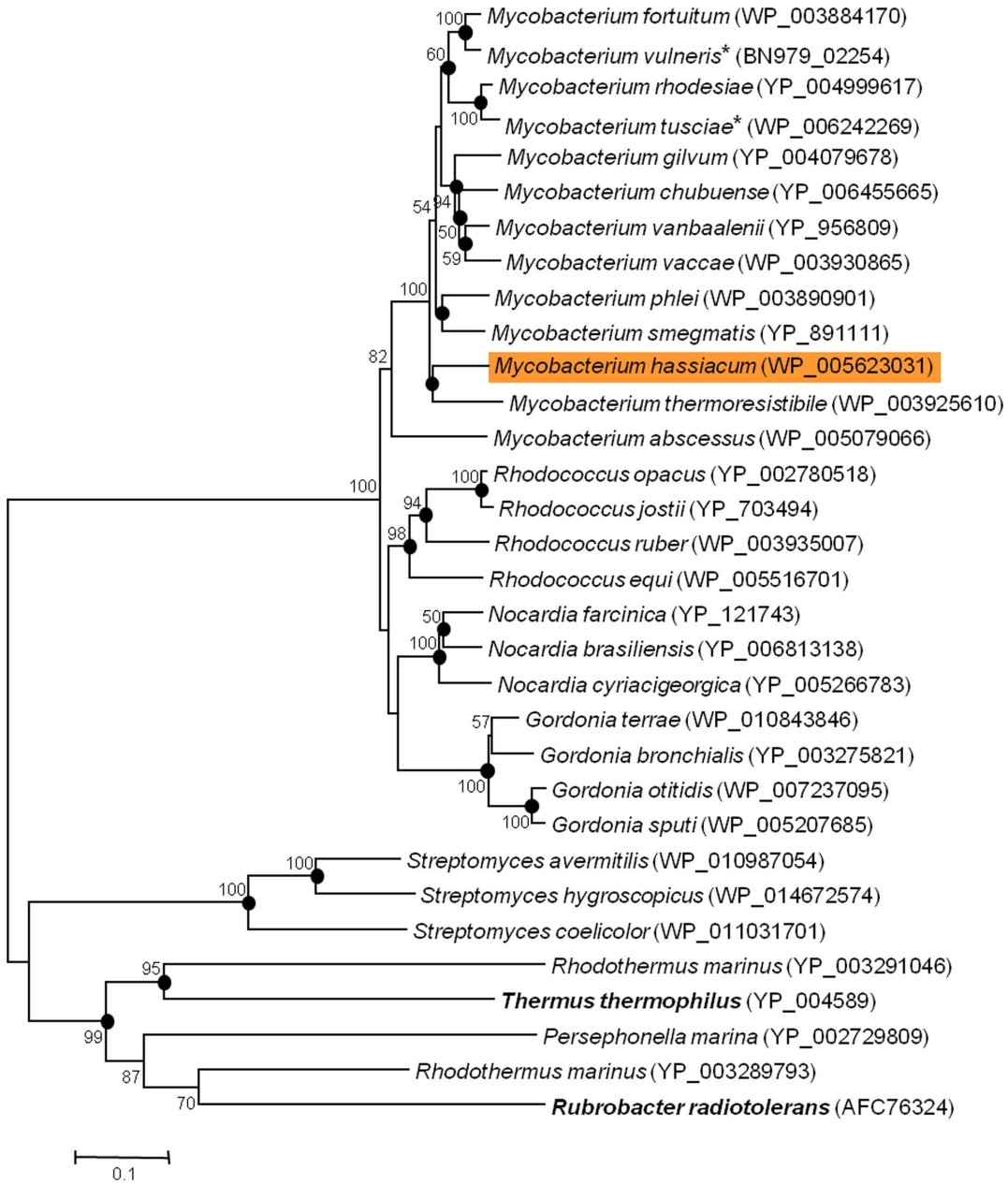

Figure 3 | Phylogenetic tree based on amino acid sequence of GgH from *M. hassiacum* (orange) and actinobacterial homologs, as well as with the orthologs from some thermophilic and halotolerant bacteria. GenPept accession numbers are indicated in parenthesis. Bold, MgHs from *T. thermophilus* HB27 and *R. radiotolerans* RSPS-4 reported to hydrolyze mannosylglycerate (MG) and GG alike[24]. *, *Mycobacterium vulneris* is a SGM and *Mycobacterium tusciae* is an ambiguous SGM/RGM where GgH orthologs have been detected. The significance of the branching order was evaluated by bootstrap analysis of 1000 computer-generated trees. The bootstrap values are indicated. Bar, 0.1 change/site. Symbol (●) indicates node branches conserved when tree was reconstructed using maximum-likelihood algorithm. Bar, 0.1 change/site.

especially due to the abundant mycolic acids, very long and branched fatty acids, either covalently attached to the arabinogalactan layer of the cell wall or to solvent-extractable trehalose-monomycolates and dimycolates[36]. In these bacteria, fatty acids biosynthesis was proposed to be modulated by two polymethylated polysaccharides (PMPSs), the methylglucose lipopolysaccharides (MGLP) and the methylmannose polysaccharides (MMP), the latter of which probably restricted to RGM[37,38]. The pathway for MGLP biosynthesis, namely polymerization of the main chain and subsequent reactions, was proposed to be initiated from glucosylglycerate (GG), an organic solute detected in *M. smegmatis* cytoplasm synthesized in two steps through a phosphorylated intermediate[15,38,39]. The first gene, coding for glucosyl-3-phosphoglycerate synthase (GpgS), was shown to be crucial for MGLP synthesis in *M. smegmatis* and growth under thermal stress but, unlike the homologue from *M. tuberculosis* (*Rv1208* in strain H37Rv), its inactivation was not lethal[20,22,23]. This apparent discrepancy was suggested to relate to the presence of both the isofunctional MGLP and MMP in the saprophyte but not in the strict pathogen, which could possibly be functionally interchangeable. The second step in the MGLP pathway was found to be catalyzed by an atypical glucosyl-3-phosphoglycerate phosphatase (GpgP, *Rv2419c* in *M. tuberculosis* H37Rv) of the histidine phosphatase superfamily that was not a sequence homolog of the isofunctional GpgPs of the HAD superfamily (EC 3.1.3.85), initially identified in other microorganisms able to synthesize GG[13,21,40]. After their identification, these two MGLP enzymes have been crystallized and their three-

Table 2 | Organisms where free GG has been detected and identification of protein sequences associated to GG biosynthesis and hydrolysis in the corresponding genome sequences

	GG synthesis					GG hydrolysis	
Organism	GpgS	GpgP* (His-Phos)	GpgP* (HAD-like)	GgS	SucP[a]	GgH	References
Mycobacterium hassiacum	●	●	○	○	○	●	This work[29]
Mycobacterium smegmatis	●	●	○	○	○	●	15
Streptomyces caelestis	-	-	-	-	-	-	31
Streptomyces lincolnensis	-	-	-	-	-	-	32
Synechococcus PCC7002	●	○	●	○	●	○	12
Procholorococcus marinus	●	○	●	○	●	○	12
Halomonas elongata[b]	●	○	●	○	●	○	60
Erwinia chrysanthemii[b]	●	○	●	○	○	○	11
Persephonella marina	●	○	●	●	○	●	61
Geodermatophilus obscurus	●	●	○	○	○	○	13
Methanohalophilus portucalensis	●	-	-	-	-	-	33,40

(●) Proteins with significant homology detected.
(○) Conserved sequences not detected.
([a]) SucP is annotated as putative sucrose phosphorylase whose homologue from *Leuconostoc mesenteroides* was shown to synthesize GG from sucrose and glycerate *in vitro*[62].
([b]) *Halomonas elongata* and *Erwinia chrysanthemii* have been re-classified as *Chromohalobacter salexigens* and *Dickeya dadanti*, respectively[13].
(*) Two types of non-homologous isofunctional GpgPs of the histidine phosphatase superfamily (His-Phos)[21] and of the Haloacid dehalogenase superfamily (HAD-like)[13].
(-), no information available.
GgH, glucosylglycerate hydrolase.

dimensional structures determined for their potential as TB targets[41,42]. MGLP seems to be ubiquitous among mycobacteria and GpgS and GpgP genes are present in all their available genomes (Table 1). Nevertheless, free GG had, so far, only been confirmed to accumulate in *M. smegmatis*[10,15].

Mycobacterium hassiacum is an opportunistic pathogen that was selected as model to study GG metabolism due to its high growth rates and biomass yields as well as from its thermophilic nature, which could facilitate biochemical studies and isolation of metabolic intermediates to understand stress responses in members of this genus[26–29]. The accumulation of GG in *M. hassiacum* resembles the pattern described for *M. smegmatis* wherein this organic solute was proposed to contribute to cell fitness during nitrogen stress adaptation[10]. In other unrelated microorganisms, namely in marine cyanobacteria as well as in a plant pathogen GG also accumulated during growth under nitrogen-limited conditions with salinity as an underlying condition[10–12,43]. Interestingly, marine cyanobacteria able to fix atmospheric nitrogen do not synthesize GG, which highlights the putative correlation between GG accumulation and nitrogen acquisition[12]. The mycobacteria-related *Streptomyces lincolnensis* and *S. calestis* have been found to accumulate GG and the latter was also confirmed to export this compound to the extracellular medium when exposed to low-level salt stress[31,32]. Since GG is the primer for MGLP biosynthesis in mycobacteria, we deemed essential to probe the mechanisms through which these organisms regulate the levels of this important compound[10].

The abrupt decrease in cytoplasmic GG during mycobacterial recovery from nitrogen deprivation was hypothesized to be the con-

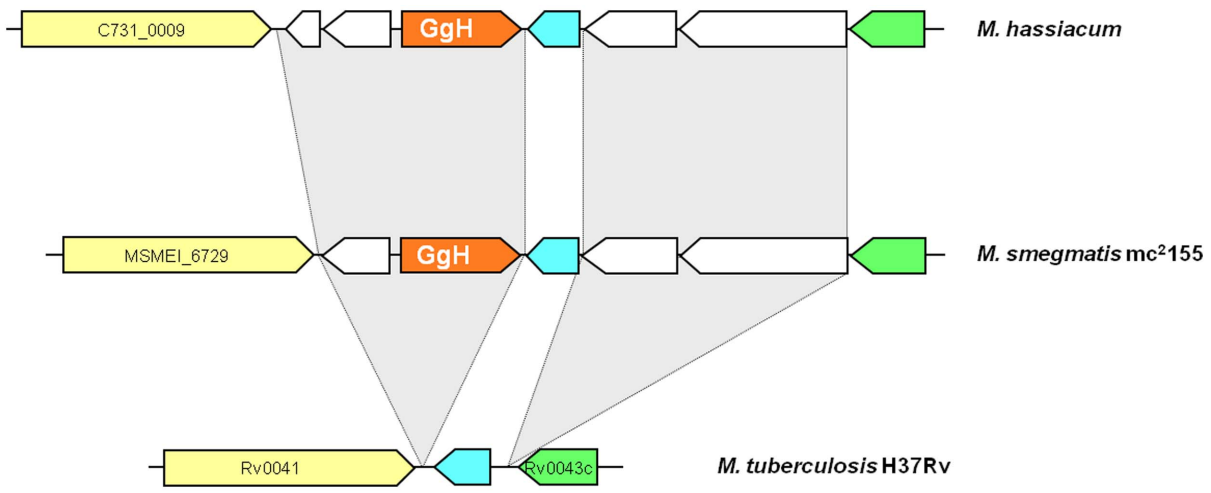

Figure 4 | Genomic organization and flanking regions of *ggH* genes (orange) from two RGM, *M. hassiacum* (C731_0006, PATRIC database) and *M. smegmatis* (MSMEI_6727), and the corresponding genomic region from *M. tuberculosis* that does not possess typical *ggH* and other three genes (white) at close range, which appear to have been lost from this pathogen's genome.

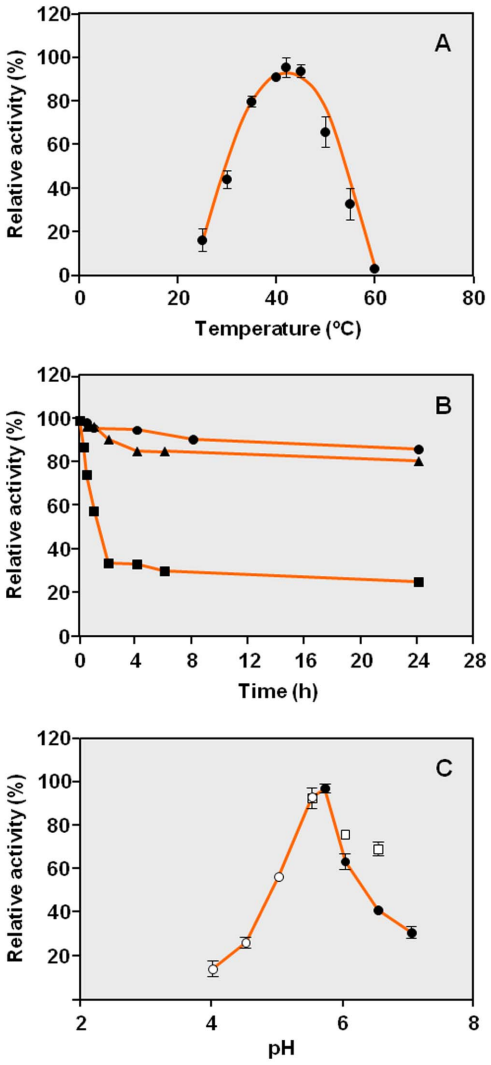

Figure 5 | Properties of the recombinant GG hydrolase (GgH) from *M. hassiacum*. (A) Temperature profile; (B) Enzyme thermostability was monitored during 24 h at 37°C (●), 42°C (▲) and 50°C (■); (C) pH dependence; enzyme activity was determined in acetate buffer (○), sodium phosphate buffer (●) and MES buffer (□). The data are the mean values of three independent experiments.

sequence of enzymatic hydrolysis and not export. While three different systems for GG synthesis have been identified in nature only in the last decade, investigation of the hydrolysis of GG has been scarce[13]. The GG-related compound mannosylglycerate (MG), often associated to osmotic stress in hyperthermophilic organisms, was recently shown to be hydrolyzed by GH63 glycoside hydrolases designated MG hydrolases (MgH)[24]. Genes coding for proteins with significant amino acid identity to MgH could be detected in mycobacterial genomes but, unlike the GG biosynthetic genes identified in all the available genomes, *mgH* homologues were, with a few exceptions, almost exclusively detected in RGM (Table 1). The characterization of the *M. hassiacum* enzyme confirmed that, unlike the MgHs from the thermophilic bacteria *Thermus thermophilus* and *Rubrobacter radiotolerans* or the eukaryotic MgH from *Selaginella moellendorffii* that hydrolyze MG and GG alike, GG was by far the preferred substrate of the *M. hassiacum* enzyme, for which we propose the designation GG hydrolase (GgH)[24,25].

Remarkably, most GG-accumulating bacteria lack GgH homologs (Table 2) for hydrolysis. Hypothetically, GG may accumulate in these organisms as a consequence of GgH absence[12,31,32]. Although the genomes of both *Streptomyces* strains found to accumulate GG are not available, the reported export to the extracellular medium may instead represent an alternative strategy to regulate the intracellular levels of this organic solute[31,32]. However, this remains hypothetical. The observation that nitrogen-starved *M. hassiacum* gradually accumulates GG during growth in a nitrogen-depleted medium and that its levels abruptly decrease upon nitrogen replenishment with concomitant up-regulation of GgH mRNA levels, clearly implicated GgH in GG catabolism *in vivo*. Furthermore, GG was not detected in the extracellular medium. Although the presence of a non-homologous GG-hydrolyzing enzyme cannot be ruled out, it is possible that in the absence of GgH, *M. tuberculosis* and other SGM may also resort to the export strategy used by *S. caelestis*, eventually to regulate GG levels.

Mycobacterium smegmatis grown under nitrogen-limiting conditions is also known to accumulate high levels of carbon/energy-rich glycogen, which has been shown to be readily mobilized when cells were transferred to nitrogen-rich medium[10,44]. Thus, the accumulation of the negatively charged GG during nitrogen stress does not appear to be an important carbon reserve and may alternatively fulfill a different metabolic role. However, while the GG accumulated during nitrogen stress in marine cyanobacteria and in *Erwinia chrysanthemi* is also driven by medium salinity to replace the nitrogen-rich glutamate that is normally accumulated as a counterion for potassium during the early stages of osmoadaptation under nitrogen-limiting conditions, the mycobacterial accumulation of GG upon nitrogen starvation has not been associated to osmoadaptation[11,12]. Hence, the molecular role of GG in the mycobacterial response to nitrogen fluctuations remains undisclosed[11,12].

One interesting feature of GgH was the apparently high K_M values for GG *in vitro*, especially when compared to the higher affinity of the related MgHs from thermophilic bacteria for both MG and GG[24]. It is

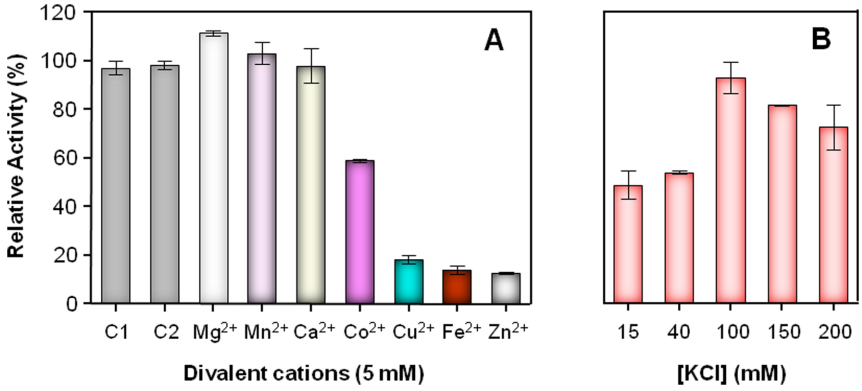

Figure 6 | (A) Effect of divalent cations on GgH activity (C1, reaction without cations; C2, reaction with 5 mM EDTA). (B) effect of KCl concentrations on GgH activity. Data are the mean values of three independent experiments.

Table 3 | Kinetic parameters of recombinant GgH from *M. hassiacum*

Temperature (°C)	Substrate	K_M (mM)	V_{max} (μmol/min.mg protein)
37	GG	16.7 ± 6.1	13.7 ± 2.6
42		16.7 ± 3.0	15.2 ± 1.5
50		11.2 ± 2.0	12.3 ± 1.0

possible that these *in vitro* measurements reflect a putative regulatory system to control intracellular GG levels when they reach the high millimolar range *in vivo*. Mycobacterial trehalases also have apparently high K_M values for trehalose (>20 mM), which is not surprising in light of the frequently high intracellular trehalose concentrations required for multiple fates in these organisms, namely as precursor for different glycolipids including the abundant cell wall trehalose dimycolates[36,45]. On the other hand, GG may be a component of unknown structures related to the GG-containing glycolipid from *Nocardia* spp. or to atypical GG-based oligosaccharides detected in hyperthermophilic bacteria. The apparently low affinity *in vitro* of GgH for GG could serve to prevent exhaustion of GG when at lower concentrations *in vivo*[13]. It is also possible that in order to maximize GG accumulation under nitrogen stress, the up-regulation of GpgS is coordinated with GgH inactivation[10]. On the other hand trehalose synthesis and hydrolysis often occur simultaneously in the mycobacterial cytoplasm and glycogen metabolism requires the constitutive activities of glycosyltransferases (synthesis) and amylases (hydrolysis)[10,45]. Hence, the possibility of GpgS and GgH concerted activity, albeit at different rates, cannot also be excluded at this stage. Although we have detected *ggH* mRNA under all conditions tested, it has not been demonstrated if GgH is active at all stages of acclimation to nitrogen stress.

The genomic organization around *ggH* seems to suggest that this gene was lost from *M. tuberculosis* and from other SGM, in agreement with phylogenetic data arguing that RGM evolutionarily precede SGM[46]. Moreover, additional genes in the *ggH* genomic region also appear to have been lost during *M. tuberculosis* evolution to the human niche (Fig. 4)[3]. This appears to indicate that the regulatory circuit driving GG accumulation as response to nitrogen starvation and depletion upon nitrogen assimilation is not required by *M. tuberculosis* for survival within its host. The investigation of GG accumulation and its fate within this pathogen enduring nitrogen fluctuations within macrophages and extracellularly represents an important subject for future research.

In addition to the genes for initiation of MGLP biosynthesis identified recently[20,21], this important pathway should also accommodate GgH (Fig. 8) as a possible regulatory step of MGLP biosynthesis

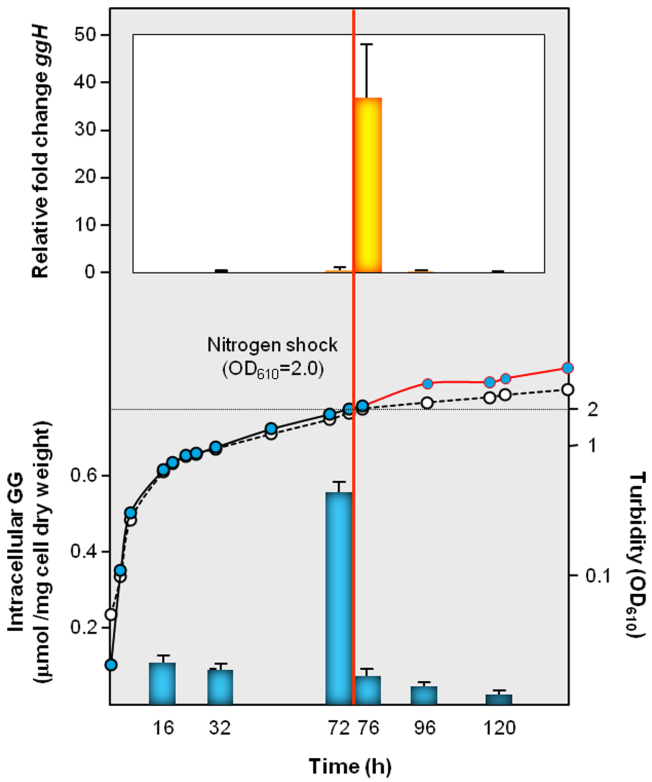

Figure 7 | Upper panel, relative expression profile (fold change) of the *ggH* gene normalized to the *rpoB* reference gene. Each point represents the mean value of three independent experiments (n = 3) performed upon sample triplicates. Bottom panel, levels of intracellular GG accumulated during growth of *M. hassiacum* under nitrogen stress followed by the addition of 10 mM ammonium sulphate. Sampling points are indicated in Figure 1.

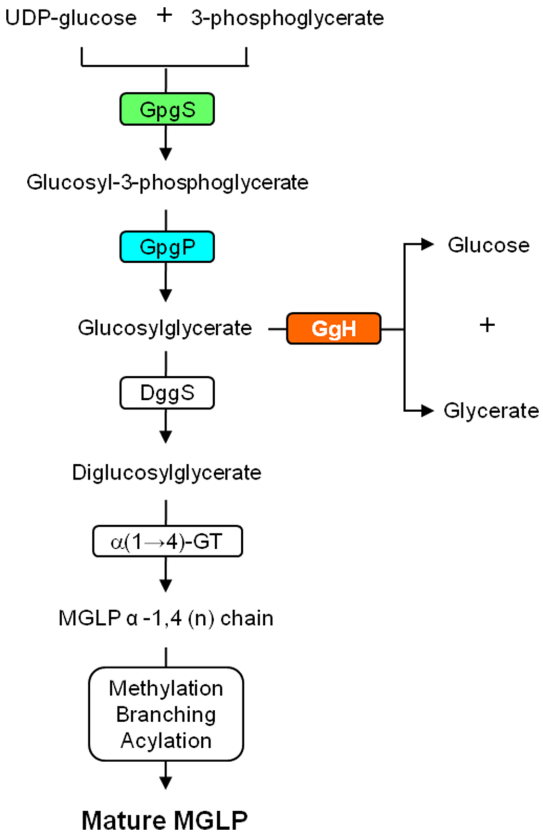

Figure 8 | Schematic representation of the proposed pathway for MGLP biosynthesis in rapidly-growing mycobacteria now including the GG-hydrolyzing activity (GgH) characterized in this study and which is absent from most slowly-growing mycobacteria. GpgS, glucosyl-3-phosphoglycerate synhase[20]; GpgP, glucosyl-3-phosphoglycerate phosphatase[21]; GgH, glucosylglycerate hydrolase; DggS, putative diglucosylglycerate synthase; α(1 → 4)-GT, glycosyltransferase. Some of the subsequent steps (white) have been genetically associated to the cluster comprising Rv3030 to Rv3037c in *M. tuberculosis* H37Rv[37,55].

during growth of RGM under nitrogen stress. The findings reported here appear to link nitrogen stress to fatty acids homeostasis through GG metabolism and open new avenues for research into the cross-regulation of these essential pathways that may ultimately contribute to the mycobacterial resilience to environmental stress and help establish long-term infections.

Methods

Strains and growth conditions. *Mycobacterium hassiacum* DSM 44199 (DSMZ, Germany) was grown at 50°C in a glycerol-based GPHF medium (DSMZ 553) supplemented with 0.2% Tween 80. The nitrogen-limited medium was Middlebrook 7H9 adjusted to pH 7.2 and without sodium citrate, L-glutamic acid and copper sulfate; ferric ammonium citrate was replaced by ferric citrate. The nitrogen source was 1 mM ammonium sulphate ($(NH_4)_2SO_4$). Glycerol (8 mL/L) and 0.2% Tween 80 were added. Growth was monitored at 610 nm for 7 days at 50°C in metal-capped flasks containing 200 mL of medium, with continuous aeration and stirred at 150 rpm. The nitrogen shock was performed with the addition of 10 mM ammonium sulphate at an $OD_{610nm} \sim 2.0$, 72 h growth. Aliquots were harvested at appropriate times for quantification of glucosylglycerate (GG) levels and cell dry weight, and to examine the relative expression of *ggH* gene by RT-qPCR. Sampling was carried out at $OD_{610nm} = 0.5$, 1.0 and 2.0 before the nitrogen shock, and at 4, 24 and 48 h after ammonium replenishment (Fig. S1).

Quantification of GG. 100 mL aliquots were collected at different times and used for extraction of organic solutes with boiling ethanol as previously described[40]. GG was quantified with the recombinant MgH from *Rubrobacter radiotolerans* as previously described[24], and with the *M. hassiacum* GgH (20 μg) in standard reaction mixtures, incubated overnight at 42°C to ensure complete GG hydrolysis. Appropriate calibration curves with known amounts of GG (0–40 μg) were performed. Products were analyzed by thin-layer chromatography (TLC) (Silica Gel 60, Merck) with chloroform/methanol/acetic acid/water (30 : 50 : 8 : 4, v/v/v/v) and visualized after α-naphthol/sulphuric acid staining at 120°C[47]. To determine cell dry weight 50 mL culture aliquots were harvested by centrifugation (8000 rpm, 10 min), the cell pellets washed twice with cold water and dried at 50°C.

Identification of glucosylglycerate hydrolase and phylogenetic analyses. The identification of glucosylglycerate hydrolase genes (*ggH*) was carried out with BLAST using amino acid sequences of mannosylglycerate hydrolases (MgH) from *T. thermophilus* and *R. radiotolerans*[24]. The amino acid sequence of the putative glucosylglycerate hydrolase (GgH) from *M. hassiacum* DSM 44199 was retrieved from the genome sequence available at the PATRIC (http://wwww.patricbrc.org/) database and used for alignments with GgH orthologs obtained from NCBI and KEGG (http://www.genome.jp/kegg/) databases, using BioEdit Sequence Alignment Editor[29,48]. The phylogenetic tree was generated with MEGA5.2 software and constructed using neighbor-joining and maximum-likelihood included in MEGA 5.2 algorithms[49–51].

Cloning. *M. hassiacum* DNA was isolated with a protocol adapted from Nielsen and colleagues[52] with initial incubation for 2 h in GTE buffer (50 mM glucose, 25 mM Tris-HCl at pH 8.0 and 10 mM EDTA) containing lysozyme (20 mg/mL), at 37°C. The *ggH* gene was amplified with primers GgHF 5′-AATTGAGTCATATGCC-GCACGACCCGAGTT and GgHR 5′-CATAAGCTTGCCCAGCCAGTCG-AGCAC, with NdeI and HindIII restriction sites (underlined), respectively. The stop codon was removed to allow translation of a C-terminal 6 × His tag from pET30a vector. PCR was carried out with KOD Hot-Start DNA polymerase (Novagen) and the product was cloned between NdeI and HindIII sites of pET30a and transformed into *E. coli* BL21[20].

Overexpression of *ggH* and purification of GgH. *E. coli* cells containing the recombinant plasmid were grown to mid-exponential phase ($OD_{610nm} = 0.8$) at 37°C in baffled 1-L erlenmeyer flasks containing 300 mL of LB medium at pH 7.0 supplemented with kanamycin (30 μg/mL). Expression was induced with 0.4 mM IPTG and growth was allowed to proceed for 18 h at 25°C. Cells were harvested, suspended in 20 mM sodium phosphate buffer at pH 7.5 (buffer A) containing 2 mg/mL DNAseI and 5 mM $MgCl_2$, disrupted by sonication and centrifuged (15000 rpm, 15 min, 4°C) to remove cell debris.

The His-tagged recombinant GgH was purified in a FPLC system (GE Healthcare), with a Ni-Sepharose column equilibrated with buffer A containing 0.5 M NaCl and 20 mM imidazole. Elution was carried out with buffer A containing 0.5 M NaCl and 500 mM imidazole (buffer B). The purest active fractions were pooled, concentrated, equilibrated with buffer A containing 200 mM KCl for stabilization and stored on ice[24]. The protein content was determined with a Bradford assay kit (BioRad). The extent of oligomerization of pure recombinant GgH was estimated as previously described[21].

Chemical synthesis of GG. Glucosylglycerate (GG, α-glucosyl-D-glycerate) was synthesized as previously described[53]. Following the same synthetic strategy but using the L-glycerate derivative as the glycosyl acceptor in the glycosylation reaction, α-glucosyl-L-glycerate was obtained. In a similar way, but varying the hexose as the glycosyl donor and the alcohol as the glycosyl acceptor, eight new synthetic GG analogues were prepared and the protocols will be described elsewhere (M. R. Ventura, personal communication).

GgH activity assay and substrate specificity. Substrate specificity of GgH was examined at 42°C for 1 h in 50 μL mixtures containing pure enzyme (10 μg), 25 mM sodium phosphate buffer at pH 6.0, 5 mM $MgCl_2$, 100 mM KCl and 10 mM of each of the following substrates: glucosylglycerate (GG), mannosylglycerate (MG), glucosylglycerol, trehalose, sucrose, isomaltose and diglucosylglycerate. To test for possible transglucosylation reactions, standard mixtures containing 50 to 200 mM GG alone or with 50 mM glucose were incubated overnight at 42°C with 10 μg of pure GgH. Products were visualized by TLC as described above. 4-nitrophenyl-α-D-glucopyranoside and 4-nitrophenyl-β-D-glucopyranoside were also tested as possible substrates by monitoring the increase in absorbance at 410 nm[24].

Biochemical characterization and kinetic parameters. The temperature profile and thermal stability of GgH, the effect of pH, cation dependence and effects of salt were calculated from the glucose released. Standard reaction conditions were 10 mM GG, 100 mM KCl, the appropriate buffer and cation in a volume of 50 μL. Mixtures were pre-heated for 2 min, reactions initiated by addition of GgH (6.4 μg) and stopped at appropriate times (up to 8 min) by cooling on ethanol-ice. All reactions were performed in triplicate.

The effect of pH was determined in standard conditions at 42°C in buffers 25 mM acetate (pH 4.0–5.5), 25 mM citrate-phosphate (pH 2.6–5.0), 25 mM MES (pH 5.5–6.5) or 25 mM sodium phosphate (pH 5.8–7.0) (5 to 20 mM sodium phosphate buffer at pH 5.8 were also tested) containing 5 mM $MgCl_2$. Temperature profile was determined between 25°C and 60°C with 16 mM sodium phosphate buffer at pH 5.8 and 5 mM $MgCl_2$. The effect of cations was examined by addition of 5 mM of the chloride salts of Mg^{2+}, Mn^{2+}, Co^{2+}, Ca^{2+}, Fe^{2+}, Zn^{2+} and Cu^{2+}. Reactions without cations or with 5 mM EDTA were the negative controls. The effect of KCl concentration was tested by addition of 15 to 200 mM KCl to standard mixtures. Thermal stability was determined by incubating GgH (30 μL of a solution at 3.2 μg/μL) in 25 mM sodium phosphate buffer (pH 6.0) containing 100 mM KCl at 37, 42 and 50°C. Samples were cooled on ice at different times and residual activity examined under optimal conditions.

Kinetic parameters were determined under optimum reaction conditions, in mixtures containing 6.4 μg of GgH and variable concentrations of GG. K_M and V_{max} were determined with GraphPad Prism software (version 5.00), where the Michaelis-Menten equation was used. All experiments were performed in triplicate.

RNA extraction. During *M. hassiacum* growth in nitrogen-restricted medium, 3 mL aliquots were collected at different sampling points, centrifuged (13500 rpm, 5 min, 4°C) and the pellets stored at −80° C. To maximize cells lysis, an initial step of 5 cycles of 30 seconds each using MagNA Lyser Green Beads (Roche) at 4000 rpm was introduced in the RNA isolation kit (NZYTech) protocol. On-column DNase treatment was optimized using the RapidOut DNA Removal Kit (Thermo Scientific) with a 90 min incubation. RNA integrity was verified on agarose gel and concentration and purity were determined with a Nanodrop ND-1000 spectrophotometer.

Reverse transcription quantitative real-time PCR (RT-qPCR). Primers 5′-GCAA-GGGATTTCGATGTGCT and 5′-ATCAGCCCGTACTTCAGGTC for the target *ggH* gene were designed using Primer 3 software®. The *rpoB* gene was used as reference for normalization control and the primer sequences were 5′-GACGACA-TCGACCACTTCGG and 5′-GGGGTCTCGATCGGGCACAT[54]. RNA samples were normalized to 10 ng/μL that were synthesized into first strand cDNA using iScript Select cDNA synthesis kit (BioRad Laboratories). For each sample 500 nM of reverse primer was used in a 20 μL reaction. The efficiency of each pair of primers was tested using the resulting cDNA diluted in 5 series of 5-fold dilutions (starting from 20 ng/μL). Standard curves were constructed and the slope was used to calculate primers efficiency.

The expression of *ggH* was determined by RT-qPCR on a Bio-Rad CFX96™ Real-time PCR system. A reaction mix was prepared in triplicate using 5 μL of cDNA and 500 nM of each forward and reverse primer in a total volume of 20 μL following the protocol for the SsoFast™ Evagreen® Supermix kit (BioRad Laboratories). The amplification reaction conditions included an initial denaturation at 95°C for 30 s followed by 50 cycles (95°C for 5 s and 69°C for 10 s) and melting curve analysis (65–95°C with plate readings every 0.5°C) to confirm amplification specificity. The expected sizes of 365 bp for *rpoB* and 167 bp for *ggH*, were verified on a 1.5% agarose gel. To check for primer and genomic DNA contamination controls were included: NTC (No Template Control) and No-RT (No Reverse Transciptase).

The relative expression of *ggH* was analyzed with the Livak method in which the relation between the Ct values of the target and reference gene was considered. The values of the relative expression of *ggH* were calculated using the formula $2^{-\Delta\Delta Ct}$ [35]. In this study the ΔCt was calculated as the difference between the Ct value with the *ggH* primers and the Ct value with the *rpoB* primers. The ΔΔCt was obtained from the difference between the ΔCt value of the nitrogen-shocked cells and the ΔCt value of the cells grown without the nitrogen shock.

1. Fowler, D. *et al.* The global nitrogen cycle in the twenty-first century. *Philos Trans R Soc Lond B Biol Sci* **368**, 20130164 (2013).

2. Williams, K. J. *et al.* Deciphering the response of *Mycobacterium smegmatis* to nitrogen stress using bipartite active modules. *BMC Genomics* **14**, 436 (2013).
3. Amon, J., Titgemeyer, F. & Burkovski, A. A genomic view on nitrogen metabolism and nitrogen control in mycobacteria. *J Mol Microbiol Biotechnol* **17**, 20–9 (2009).
4. Gtari, M., Ghodhbane-Gtari, F., Nouioui, I., Beauchemin, N. & Tisa, L. S. Phylogenetic perspectives of nitrogen-fixing actinobacteria. *Arch Microbiol* **194**, 3–11 (2012).
5. Sellstedt, A. & Richau, K. H. Aspects of nitrogen-fixing Actinobacteria, in particular free-living and symbiotic Frankia. *FEMS Microbiol Lett* **342**, 179–86 (2013).
6. Falkinham, J. O., 3rd. Surrounded by mycobacteria: nontuberculous mycobacteria in the human environment. *J Appl Microbiol* **107**, 356–67 (2009).
7. Nessar, R., Cambau, E., Reyrat, J. M., Murray, A. & Gicquel, B. *Mycobacterium abscessus*: a new antibiotic nightmare. *J Antimicrob Chemother* **67**, 810–8 (2012).
8. Primm, T. P., Lucero, C. A. & Falkinham, J. O., 3rd. Health impacts of environmental mycobacteria. *Clin Microbiol Rev* **17**, 98–106 (2004).
9. Leigh, J. A. & Dodsworth, J. A. Nitrogen regulation in bacteria and archaea. *Annu Rev Microbiol* **61**, 349–77 (2007).
10. Behrends, V., Williams, K. J., Jenkins, V. A., Robertson, B. D. & Bundy, J. G. Free glucosylglycerate is a novel marker of nitrogen stress in *Mycobacterium smegmatis*. *J Proteome Res* **11**, 3888–96 (2012).
11. Goude, R., Renaud, S., Bonnassie, S., Bernard, T. & Blanco, C. Glutamine, glutamate, and alpha-glucosylglycerate are the major osmotic solutes accumulated by *Erwinia chrysanthemi* strain 3937. *Appl Environ Microbiol* **70**, 6535–41 (2004).
12. Klahn, S., Steglich, C., Hess, W. R. & Hagemann, M. Glucosylglycerate: a secondary compatible solute common to marine cyanobacteria from nitrogen-poor environments. *Environ Microbiol* **12**, 83–94 (2010).
13. Empadinhas, N. & da Costa, M. S. Diversity, biological roles and biosynthetic pathways for sugar-glycerate containing compatible solutes in bacteria and archaea. *Environ Microbiol* **13**, 2056–77 (2011).
14. Saier, M. H., Jr. & Ballou, C. E. The 6-O-methylglucose-containig lipopolysaccharide of *Mycobacterium phlei*. Complet structure of the polysaccharide. *J Biol Chem* **243**, 4332–41 (1968).
15. Kamisango, K., Dell, A. & Ballou, C. E. Biosynthesis of the mycobacterial *O*-methylglucose lipopolysaccharide. Characterization of putative intermediates in the initiation, elongation, and termination reactions. *J Biol Chem* **262**, 4580–6 (1987).
16. Lee, Y. C. Isolation and characterization of lipopolysaccharides containing 6-*O*-methyl-D-glucose from *Mycobacterium* species. *J Biol Chem* **241**, 1899–908 (1966).
17. Lee, Y. C. & Ballou, C. E. 6-O-Methyl-D-Glucose from Mycobacteria. *J Biol Chem* **239**, PC3602–3 (1964).
18. Ilton, M. *et al.* Fatty acid synthetase activity in *Mycobacterium phlei*: regulation by polysaccharides. *Proc Natl Acad Sci U S A* **68**, 87–91 (1971).
19. Gray, G. R. & Ballou, C. E. Isolation and characterization of a polysaccharide containing 3-*O*-methyl-D-mannose from *Mycobacterium phlei*. *J Biol Chem* **246**, 6835–42 (1971).
20. Empadinhas, N., Albuquerque, L., Mendes, V., Macedo-Ribeiro, S. & da Costa, M. S. Identification of the mycobacterial glucosyl-3-phosphoglycerate synthase. *FEMS Microbiol Lett* **280**, 195–202 (2008).
21. Mendes, V., Maranha, A., Alarico, S., da Costa, M. S. & Empadinhas, N. *Mycobacterium tuberculosis* Rv2419c, the missing glucosyl-3-phosphoglycerate phosphatase for the second step in methylglucose lipopolysaccharide biosynthesis. *Sci Rep* **1**, 177 (2011).
22. Kaur, D. *et al.* Initiation of methylglucose lipopolysaccharide biosynthesis in mycobacteria. *PLoS One* **4**, e5447 (2009).
23. Griffin, J. E. *et al.* High-resolution phenotypic profiling defines genes essential for mycobacterial growth and cholesterol catabolism. *PLoS Pathog* **7**, e1002251 (2011).
24. Alarico, S., Empadinhas, N. & da Costa, M. S. A new bacterial hydrolase specific for the compatible solutes alpha-D-mannopyranosyl-(1-->2)-D-glycerate and alpha-D-glucopyranosyl-(1-->2)-D-glycerate. *Enzyme Microb Technol* **52**, 77–83 (2013).
25. Nobre, A. *et al.* The plant *Selaginella moellendorffii* possesses enzymes for synthesis and hydrolysis of the compatible solutes mannosylglycerate and glucosylglycerate. *Planta* **237**, 891–901 (2013).
26. Jiang, S. H., Roberts, D. M., Clayton, P. A. & Jardine, M. Non-tuberculous mycobacterial PD peritonitis in Australia. *Int Urol Nephrol* **45**, 1423–8 (2013).
27. Schroder, K. H., Naumann, L., Kroppenstedt, R. M. & Reischl, U. *Mycobacterium hassiacum* sp. nov., a new rapidly growing thermophilic mycobacterium. *Int J Syst Bacteriol* **47**, 86–91 (1997).
28. Tortoli, E., Reischl, U., Besozzi, G. & Emler, S. Characterization of an isolate belonging to the newly described species *Mycobacterium hassiacum*. *Diagn Microbiol Infect Dis* **30**, 193–6 (1998).
29. Tiago, I. *et al.* Genome sequence of *Mycobacterium hassiacum* DSM 44199, a rare source of heat-stable mycobacterial proteins. *J Bacteriol* **194**, 7010–1 (2012).
30. Cantarel, B. L. *et al.* The Carbohydrate-Active EnZymes database (CAZy): an expert resource for Glycogenomics. *Nucleic Acids Res* **37**, D233–8 (2009).
31. Pospisl, S., Halada, P., Petricek, M. & Sedmera, P. Glucosylglycerate is an osmotic solute and an extracellular metabolite produced by *Streptomyces caelestis*. *Folia Microbiol (Praha)* **52**, 451–6 (2007).
32. Sedmera, P., Halada, P. & Pospisil, S. New carbasugars from *Streptomyces lincolnensis*. *Magn Reson Chem* **47**, 519–22 (2009).
33. Robertson, D. E., Lai, M. C., Gunsalus, R. P. & Roberts, M. F. Composition, Variation, and Dynamics of Major Osmotic Solutes in *Methanohalophilus* Strain FDF1. *Appl Environ Microbiol* **58**, 2438–43 (1992).
34. Taylor, S., Wakem, M., Dijkman, G., Alsarraj, M. & Nguyen, M. A practical approach to RT-qPCR-Publishing data that conform to the MIQE guidelines. *Methods* **50**, S1–5 (2010).
35. Schmittgen, T. D. & Livak, K. J. Analyzing real-time PCR data by the comparative C(T) method. *Nat Protoc* **3**, 1101–8 (2008).
36. Nobre, A., Alarico, S., Maranha, A., Mendes, V. & Empadinhas, N. The molecular biology of mycobacterial trehalose in the quest for advanced tuberculosis therapies. *Microbiology* (2014).
37. Jackson, M. & Brennan, P. J. Polymethylated polysaccharides from *Mycobacterium* species revisited. *J Biol Chem* **284**, 1949–53 (2009).
38. Mendes, V., Maranha, A., Alarico, S. & Empadinhas, N. Biosynthesis of mycobacterial methylglucose lipopolysaccharides. *Nat Prod Rep* **29**, 834–44 (2012).
39. Forsberg, L. S., Dell, A., Walton, D. J. & Ballou, C. E. Revised structure for the 6-*O*-methylglucose polysaccharide of *Mycobacterium smegmatis*. *J Biol Chem* **257**, 3555–63 (1982).
40. Costa, J. *et al.* Characterization of the biosynthetic pathway of glucosylglycerate in the archaeon *Methanococcoides burtonii*. *J Bacteriol* **188**, 1022–30 (2006).
41. Pereira, P. J. *et al. Mycobacterium tuberculosis* glucosyl-3-phosphoglycerate synthase: structure of a key enzyme in methylglucose lipopolysaccharide biosynthesis. *PLoS One* **3**, e3748 (2008).
42. Zheng, Q. *et al.* On mechanism of dephosphorylation of glucosyl-3-phosphoglycerate by a histidine phosphatase. *J Biol Chem* (2014).
43. Kollman, V. H., Hanners, J. L., London, R. E., Adame, E. G. & Walker, T. E. Photosynthetic preparation and characterization of 13C-labeled carbohydrates in *Agmenellum quadruplicatum*. *Carbohydr Research* **73**, 9 (1979).
44. Elbein, A. D. & Mitchell, M. Levels of glycogen and trehalose in *Mycobacterium smegmatis* and the purification and properties of the glycogen synthetase. *J Bacteriol* **113**, 863–73 (1973).
45. Carroll, J. D., Pastuszak, I., Edavana, V. K., Pan, Y. T. & Elbein, A. D. A novel trehalase from *Mycobacterium smegmatis* - purification, properties, requirements. *FEBS J* **274**, 1701–14 (2007).
46. Devulder, G., Perouse de Montclos, M. & Flandrois, J. P. A multigene approach to phylogenetic analysis using the genus *Mycobacterium* as a model. *Int J Syst Evol Microbiol* **55**, 293–302 (2005).
47. Jacin, H. & Mishkin, A. R. Separation of Carbohydrates on Borate-Impregnated Silica Gel G Plates. *J Chromatogr* **18**, 170–3 (1965).
48. Hall, T. A. BioEdit: a user-friendly biological sequence alignment editor and analysis program for Windows 95/98/NT. *Nucl. Acids. Symp. Ser.* **41**, 4 (1999).
49. Tamura, K. *et al.* MEGA5: molecular evolutionary genetics analysis using maximum likelihood, evolutionary distance, and maximum parsimony methods. *Mol Biol Evol* **28**, 2731–9 (2011).
50. Saitou, N. & Nei, M. The neighbor-joining method: a new method for reconstructing phylogenetic trees. *Mol Biol Evol* **4**, 406–25 (1987).
51. Olsen, G. J., Matsuda, H., Hagstrom, R. & Overbeek, R. fastDNAmL: a tool for construction of phylogenetic trees of DNA sequences using maximum likelihood. *Comput Appl Biosci* **10**, 41–8 (1994).
52. Nielsen, P., Fritze, D. & Priest, F. G. Phenetic diversity of alkaliphilic *Bacillus* strains: proposal for nine new species. *Microbiology* **141**, 16 (1995).
53. Lourenco, E. C., Maycock, C. D. & Ventura, M. R. Synthesis of potassium (2R)-2-O-a-D-glucopyranosyl-(1->6)-a-D-glucopyranosyl-2,3-dihydroxypropanoate a natural compatible solute. *Carbohydr Res* **344**, 2073–2078 (2009).
54. Badejo, A. C., Badejo, A. O., Shin, K. H. & Chai, Y. G. A gene expression study of the activities of aromatic ring-cleavage dioxygenases in *Mycobacterium gilvum* PYR-GCK to changes in salinity and pH during pyrene degradation. *PLoS One* **8**, e58066 (2013).
55. Stadthagen, G. *et al.* Genetic basis for the biosynthesis of methylglucose lipopolysaccharides in *Mycobacterium tuberculosis*. *J Biol Chem* **282**, 27270–6 (2007).
56. Tuffal, G., Albigot, R., Riviere, M. & Puzo, G. Newly found 2-N-acetyl-2,6-dideoxy-beta-glucopyranose containing methyl glucose polysaccharides in *M. bovis* BCG: revised structure of the mycobacterial methyl glucose lipopolysaccharides. *Glycobiology* **8**, 675–84 (1998).
57. Hunter, S. W., Gaylord, H. & Brennan, P. J. Structure and antigenicity of the phosphorylated lipopolysaccharide antigens from the leprosy and tubercle bacilli. *J Biol Chem* **261**, 12345–51 (1986).
58. Tuffal, G., Ponthus, C., Picard, C., Riviere, M. & Puzo, G. Structural elucidation of novel methylglucose-containing polysaccharides from *Mycobacterium xenopi*. *Eur J Biochem* **233**, 377–83 (1995).
59. Weisman, L. S. & Ballou, C. E. Biosynthesis of the mycobacterial methylmannose polysaccharide. Identification of an alpha 1----4-mannosyltransferase. *J Biol Chem* **259**, 3457–63 (1984).
60. Canovas, D. *et al.* Role of Ngamma-acetyldiaminobutyrate as an enzyme stabilizer and an intermediate in the biosynthesis of hydroxyectoine. *Appl Environ Microbiol* **65**, 3774–9 (1999).

61. Lamosa, P. *et al.* Organic solutes in the deepest phylogenetic branches of the Bacteria: identification of alpha(1–6)glucosyl-alpha(1–2)glucosylglycerate in *Persephonella marina*. *Extremophiles* **17**, 137–46 (2013).
62. Sawangwan, T., Goedl, C. & Nidetzky, B. Glucosylglycerol and glucosylglycerate as enzyme stabilizers. *Biotechnol J* **5**, 187–91 (2010).

Acknowledgments

We are grateful to the Mizutani Foundation for Glycoscience, Japan, for financial support through the Exploratory Grant 120123. We thank Dr. Igor Tiago for invaluable support on the construction and analysis of the phylogenetic tree. This work was supported by national funds through Fundação para a Ciência e a Tecnologia (FCT) and by EU-FEDER funding through the Operational Competitiveness Programme – COMPETE (Grants FCOMP-01-0124-FEDER-014321 [PTDC/BIA-PRO/110523/2009], FCOMP-01-0124-FEDER-028359 [PTDC/BIA-MIC/2779/2012], and FCOMP-01-0124-FEDER-037276 [PEst-C/SAU/LA0001/2013-2014]. S. Alarico, A. Maranha and E. C. Lourenço acknowledge FCT fellowships SFRH/BPD/43321/2008 and SFRH/BD/74845/2010 and SFRH//BD/47702/2008.

Author contributions

S.A., M.C., M.S.S. and E.C.L. performed the experiments. S.A., M.C., M.S.S., A.M., T.Q.F. and N.E. analyzed the data. T.Q.F., M.R.V. and N.E. contributed with reagents and materials. N.E. designed the study and wrote the paper.

Additional information

Supplementary information accompanies this paper at http://www.nature.com/scientificreports

Competing financial interests: The authors declare no competing financial interests.

How to cite this article: Alarico, S. *et al. Mycobacterium hassiacum* recovers from nitrogen starvation with up-regulation of a novel glucosylglycerate hydrolase and depletion of the accumulated glucosylglycerate. *Sci. Rep.* **4**, 6766; DOI:10.1038/srep06766 (2014).